

Josephson-Kondo screening cloud in circuit quantum electrodynamics

Izak Snyman¹ and Serge Florens²

¹*Mandelstam Institute for Theoretical Physics, School of Physics,
University of the Witwatersrand, Wits, 2050, South Africa*

²*Institut Néel, CNRS and Université Grenoble Alpes, F-38042 Grenoble, France
(Dated: June 3, 2021)*

We show that the non-local polarization response in a multimode circuit-QED setup, devised from a Cooper pair box coupled to a long chain of Josephson junctions, provides an alternative route to access the elusive Kondo screening cloud. For moderate circuit impedance, we compute analytically the universal lineshape for the decay of the charge susceptibility along the circuit, that relates to spatial entanglement between the qubit and its electromagnetic environment. At large circuit impedance, we numerically find further spatial correlations that are specific to a true many-body state.

Superconducting circuits constitute at present one of the most versatile platforms for quantum engineering, due to their macroscopic - yet fully coherent - building blocks [1], offering great possibilities in tunability and design [2]. Beyond their promising use in quantum information processing, such large-scale electrical devices made out of Josephson junctions can be viewed as metamaterials [3, 4] where light-matter interactions can be explored in uncharted territory [5–9]. These systems allow for unusual physical regimes where the effective fine structure constant can become of order one [10, 11], so that ultra-strong coupling between a single two-level system and a large number of environmental modes leads to a vacuum with non-trivial entanglement properties [12]. Our aim in this Letter is to develop a simple physical picture for this massively entangled state, that we dub the Josephson-Kondo screening cloud, and to propose a realistic setup where its subtle correlations can be unveiled experimentally.

The use here of the Kondo terminology [13], usually associated to the quenching of a magnetic moment in a Fermi sea (another example of a complex many-body vacuum) may come as a surprise. However, deep connections between this purely electronic phenomenon and strongly dissipative two-level systems have been known for decades [14–16], a property which we will exploit here and further elaborate on. In fact, one challenging and still open question in the Kondo realm concerns precisely the evidence for the magnetic screening cloud, or in other words, spatial fingerprints of the entanglement structure between the localized spin and its surrounding electron bath [19–24]. Despite numerous experimental efforts [17, 18] and innovative theoretical proposals [25–29], two important difficulties are typically encountered. First, measuring weak long-range magnetic correlations is a daunting task, and an all-electrical setup would be much preferred. Second, spatial Kondo correlations show rapid $2k_F$ Friedel oscillations due scattering processes across the Fermi surface, that complicate the signal to analyze [31].

In order to bypass these difficulties, we propose in

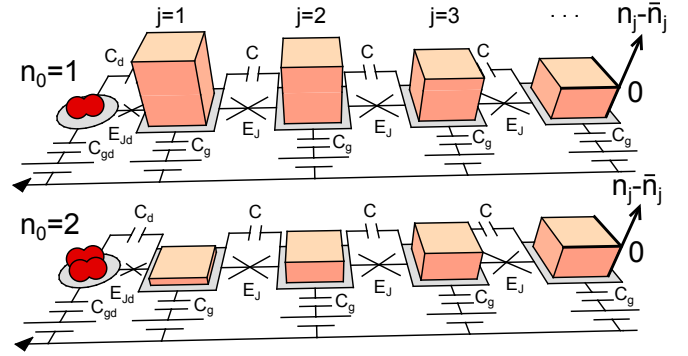


FIG. 1. (color online) Schematic view of the proposed superconducting circuit supporting two dressed qubit states, where one or two Cooper pairs in excess on the leftmost island are each accompanied by a different charge polarization cloud. Josephson tunneling between the two configurations generates entanglement between the qubit and its environment, leading to a state that possesses the same singlet structure as the magnetic Kondo screening cloud, but in the charge, rather than the spin sector.

Fig. 1 a simple all-superconducting circuit. Here, one end of a long chain of Josephson elements is coupled to a single superconducting quantum dot with a large Coulomb charging energy. The dot is tuned to a charge degeneracy point, so that the state space of the dot is reduced to two active charge levels that contain an excess of either one or two Cooper pairs. This realizes the analog of a quantized spin $1/2$ moment, but in the charge sector, which is better suited for electrical control with local gates. The low energy modes of the environment are plasmons that couple both capacitively and inductively (via Josephson tunneling) to the qubit. Quenching the charge qubit in this superconducting environment is preferable to quenching with a normal electron gas because, unlike the capacitive couplings between elements in the superconducting array, electron-electron interactions in a normal electron gas act to distort the charge screening cloud.

The interplay of charging and inductive couplings leads to the following physics. The capacitive interaction be-

tween the charge qubit and a high impedance bath generates the dressing of each of the two qubit states by a distinct charge polarization cloud, as depicted in Fig. 1. The Josephson coupling, rooted in quantum tunneling, forces in first approximation a quantum superposition of these two dressed qubit states, leading to non-trivial entanglement between the qubit and the bath. The spatial correlations of this polarization cloud can then be probed by modulating a comb of local gates applied along the chain, while recording the charge response of the two-level system. Qubit measurements can be performed by weakly coupling the qubit to a superconducting resonator. We will show that such measurements allow one to map precisely the usual magnetic Kondo screening cloud correlations, averaged over fluctuations on the scale of the Fermi wavelength. This bypasses the issue of the $2k_F$ oscillations mentioned above. A final key aspect pertaining to Kondo physics is universality, namely that phenomena beyond a model-specific short distance cut-off are insensitive to microscopic details. At low to moderate impedance, we will analytically compute the full spatial dependence of the Josephson-Kondo screening cloud, and demonstrate its universality beyond the first few sites of the array. For large dissipation (circuit impedance roughly larger than half the resistance quantum), we will numerically calculate the universal cloud, using a recently developed technique based on a generic coherent state description of environmental wavefunctions, and find that it only depends on the dissipation strength and the Kondo length.

Model. At temperatures well below the superconducting transition temperature, the proposed Josephson circuit is fully governed by the dynamics of conjugate phase ϕ_i and charge n_i degrees of freedom on the various nodes i of the array, and obeys to the following Hamiltonian

$$H = \frac{(2e)^2}{2} \sum_{i,j=0}^N (n_i - \bar{n}_i) (\hat{C}^{-1})_{ij} (n_j - \bar{n}_j) + \frac{E_J}{2} \sum_{i=1}^{N-1} (\phi_i - \phi_{i+1})^2 - E_{Jd} \cos(\phi_0 - \phi_1), \quad (1)$$

with \bar{n}_i the average number of Cooper pairs on island i , $N+1$ the total number of islands, and the commutation relation $[\phi_j, n_{j'}] = i\delta_{jj'}$ (we set $\hbar = 1$ in what follows). The matrix \hat{C} contains on-site capacitances $C_{00} = C_{gd} + C_d$, $C_{11} = C_g + C_d + C$, $C_{ii} = C_g + 2C$, $i \geq 2$, on the diagonal, as well as nearest neighbor capacitances $C_{01} = C_{10} = -C_d$, $C_{i,i+1} = C_{i+1,i} = -C$, $i \geq 1$ [32]. All other entries of \hat{C} are zero. We assumed that the charging energy in the chain (for sites $i > 0$) is much smaller than the Josephson couplings, namely $(2e)^2/(2C+C_g) \ll E_J$, so that phase differences in the chain are small. We therefore expanded the Josephson terms $-E_J \cos(\phi_i - \phi_{i+1})$, $i \geq 1$, to quadratic order. We stress that the phase difference between site $i = 0$ (the dot), and site $i = 1$ of

the chain is not small. This produces the anharmonicity in the second line of Eq. (1), which is responsible for the non-trivial physics that we discuss now.

A deep connection to quantum optics can be made following three standard steps [11], starting with a normal mode diagonalization of the quadratic part in Eq. (1), followed by a unitary transformation $\tilde{H} = UHU^\dagger$, with $U = e^{i(n_0 - \bar{n}_0)\phi_1}$, and finally a truncation of the Cooper pair box Hilbert space (at site $i = 0$) to two nearly degenerate states, owing to the parametrically large charging energy at the end of the chain, namely $(2e)^2/(C_{gd} + C_d) \gg E_{Jd}$ (see Supplementary Material [39] for details). Using the replacement with Pauli matrices $(n_0 - \bar{n}_0) \rightarrow \sigma_z/2$ and $e^{i\phi_0} \rightarrow \sigma^+$, and sending $N \rightarrow \infty$, this gives readily the Hamiltonian:

$$\tilde{H} = \int_0^\pi dk \left[\omega_k b_k^\dagger b_k - g_k (b_k^\dagger + b_k) \frac{\sigma_z}{2} \right] - E_{Jd} \frac{\sigma_x}{2}, \quad (2)$$

$$\omega_k = 2 \sin(k/2) \sqrt{\frac{(2e)^2 E_J}{C_g + 4C \sin^2(k/2)}}, \quad (3)$$

$$g_k = \frac{1}{\sqrt{2}} \frac{C_{gd}}{C_{gd} + C_d} \frac{\omega_k}{\sin(k/2)} \sqrt{\frac{\omega_k}{2\pi E_J}} \cos[k/2 - \delta_k], \quad (4)$$

the phase shift obeying $\sin(\delta_k) = \frac{\delta l}{1+\delta l} \sin(\delta_k - k)$, with $\delta l = C_d C_{gd}/[C_g(C_d + C_{gd})]$. Under the assumptions made before on the magnitude of the capacitances, one finds that $\delta l \ll 1$, so that the phase shift is small in practice. For low frequencies $\omega \ll \sqrt{(2e)^2 E_J/C}$, we find a linear spectral density of modes $J(\omega) = 2\pi\alpha\omega$, with effective fine structure constant (see Supplementary Material [39] for a discussion on this interpretation of α)

$$\alpha = \frac{1}{2\pi} \left(\frac{C_{gd}}{C_{gd} + C_d} \right)^2 \sqrt{\frac{(2e)^2}{E_J C}}. \quad (5)$$

Protocol. The observable that characterizes the spatial profile of the screening cloud is

$$\chi_j = \langle (n_0 - \bar{n}_0)(n_j - \bar{n}_j) \rangle. \quad (6)$$

which quantifies the difference in polarization on site j of the chain, associated with the distinct charge states $n_0 - \bar{n}_0 = \pm 1/2$ of the qubit. This quantity can be extracted from frequency-dependent linear response measurements as follows. We confine ourselves to zero temperature, as a finite temperature simply introduces exponential decay beyond the thermal wavelength [36]. A small AC gate voltage $V(t) = \delta V e^{i\omega t}$ is applied at the site j of the chain, causing a perturbation $\delta H = 2eC_g(\hat{C}^{-1})_{jj}\delta V e^{i\omega t}(n_j - \bar{n}_j)$. From the Kubo formula, the linear response of the qubit charge at site 0 is $\langle n_0 - \bar{n}_0 \rangle = 2eC_g(\hat{C}^{-1})_{jj}\delta V \chi(j, \omega)$ with $\chi(j, \omega) = -i \int_0^{+\infty} dt e^{i\omega t} \langle [n_0(t), n_j(0)] \rangle$. At zero temperature if follows from the fluctuation-dissipation relation that $\chi_j = - \int_0^\infty d\omega \text{Im} \chi(j, \omega)/\pi$.

After completing the same transformations on χ_j used previously to map Hamiltonian (1) into (2), one finds from (6) the general expression for the Josephson-Kondo cloud:

$$\chi_j = \frac{1}{2} \int_0^\pi dk \theta_{jk} \left\langle \sigma_z \frac{(b_k^\dagger + b_k)}{\sqrt{2}} \right\rangle - \frac{\delta_{j1}}{4}, \quad (7)$$

$$\theta_{jk} = 4 \sqrt{\frac{E_J}{2\pi\omega_k}} \sin(k/2) \cos[k(j-1/2) - \delta_k]. \quad (8)$$

Regime of intermediate fine structure constant. For up to moderate values of the circuit impedance (typically $\alpha < 0.2$), it was shown recently [12, 33–35] that the full ground state $|\Psi\rangle$ describing the coupled qubit and Josephson chain system assumes with excellent accuracy a simple form $|\Psi\rangle = (|f\rangle|\uparrow\rangle + |-f\rangle|\downarrow\rangle)/\sqrt{2}$, where

$$|\pm f\rangle = \exp \left[\pm \int_0^\pi dk f_k (b_k^\dagger - b_k) \right] |0\rangle, \quad (9)$$

and the oscillators are displaced by:

$$f_k = \frac{1}{2} \frac{g_k}{\omega_k + \Delta_R}, \quad \Delta_R = E_{Jd} \exp \left[-2 \int_0^\pi dk f_k^2 \right]. \quad (10)$$

This provides the mathematical foundation for the physical picture shown in Fig. 1, underlying the singlet-like structure of the wavefunction, that leads to entanglement between the qubit and environmental degrees of freedom.

Substituting the ground state (9) into the Josephson-Kondo cloud polarizability (7), one finds for $j > 1$:

$$\chi_j = -\frac{\Delta_R C_{gd}}{C_{gd} + C_d} \int_0^\pi dk \frac{\cos(k/2) \cos[k(j-1/2) - \delta_k]}{2\pi \omega_k + \Delta_R}. \quad (11)$$

This expression depends on all microscopic parameters of the device. However, for j sufficiently larger than $\sqrt{C/C_g}$, one finds universal single-parameter scaling: (See the supplementary material [39] for further detail.)

$$\chi_j = -Z \operatorname{Re} \left\{ e^{-i \frac{\Delta_R}{E_0} j} \Gamma \left[0, -i \frac{\Delta_R}{E_0} j \right] \right\}, \quad (12)$$

where $\Gamma(a, z)$ is the incomplete Gamma function, $E_0 = \sqrt{(2e)^2 E_J / C_g}$, and

$$Z^{-1} = 2\pi \left(1 + \frac{C_d}{C_{gd}} \right) \frac{E_0}{\Delta_R}. \quad (13)$$

The emergence of a universal scaling form can be checked in Fig. 2 comparing the exact expression (11) to the analytical formula (12) for several values of the ratio C_g/C of the chain capacitances. Formula (12) predicts the rapid decay of correlations $\chi_j = -Z(E_0/\Delta_R)^2/j^2$ at large distances. This result is in full agreement with the known asymptotics of the magnetic Kondo screening cloud in electronic systems. This leads to the identification of E_0/Δ_R as the dimensionless Kondo length (or

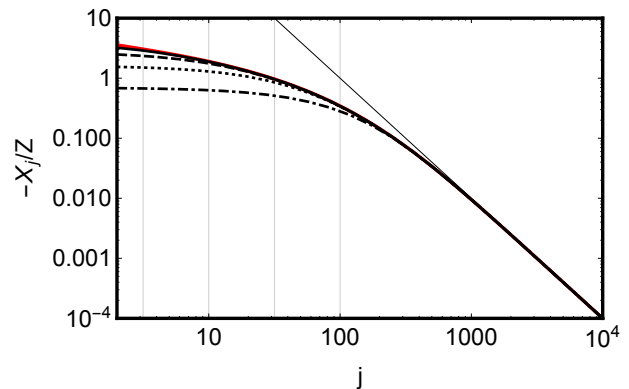


FIG. 2. Universal Josephson-Kondo cloud at intermediate values of the fine structure constant $\alpha = 0.1$. Here the exact expression (11) is computed for several choices of the capacitance ratio in the chain, $C_g/C = 10^{-4}$ (dot-dashed), $C_g/C = 10^{-3}$ (dotted), $C_g/C = 10^{-2}$ (dashed), $C_g/C = 10^{-1}$ (solid), and compared to the analytic scaling form (12). The computation is done for $E_{Jd} = E_0 = 0.01$. Vertical lines at distances $j^* = \sqrt{C/C_g} = \{\sqrt{10}, 10, \sqrt{1000}, 100\}$ indicate the cross-over between non-universal short-range and universal long-range behavior. The thin straight line indicates the long-distance asymptotic behavior $-Z\chi_j = (E_0/\Delta_R)^2/j^2$.

Kondo temperature Δ_R). The $1/j^2$ behavior may be visible in chains of several thousand sites, that can be fabricated with modern lithographic techniques. More interestingly however, the decay at intermediate distances, in the range $\sqrt{C/C_g} \ll j \ll E_J/\Delta_R$, is much slower, attesting to the stronger coupling of the qubit to the Josephson elements in its closer neighborhood. It is straightforward to see that the existence of these long-range spatial correlations are intimately connected to the strong entanglement between the qubit and its environment. Indeed, a full polarization of the qubit into the up state, even dressed by its cloud of oscillators, leads to short range correlations that do not extend beyond the second site of the chain. In addition, the long-range correlations of the Josephson-Kondo cloud also reveal the non-linearity of the Josephson element coupling site $i = 0$ and site $i = 1$. A purely harmonic chain (see Supplementary Material [39]) leads to much faster decaying correlations. The Josephson-Kondo cloud is therefore an experimentally accessible hallmark of the strong coupling between a two-level system and its macroscopic environment.

Regime of large fine structure constant. For circuit impedances close to the quantum value h/e^2 , the matter-light interaction parameter α becomes of order one, and the wavefunction (9) is in principle not sufficient. It was shown recently [37] that the non-trivial many-body ground state at large dissipation can be captured by a systematic expansion in terms of coherent states, that simply generalizes the previous ansatz to a superposition of M_{cs} coherent states $|\Psi\rangle = \sum_{n=1}^{M_{cs}} p_n |\Psi_n\rangle$, where

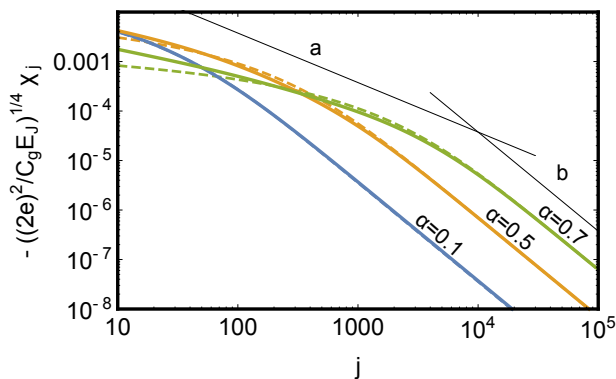


FIG. 3. Universal Josephson-Kondo cloud at increasing values of the dissipation strength α . Fully converged curves (solid lines) were obtained with $M_{cs} = 7$ coherent states. The curves were obtained at the following values of the Kondo energy: $\Delta_R = 4 \times 10^{-2} E_0$ at $\alpha = 0.1$, $\Delta_R = 4 \times 10^{-3} E_0$ at $\alpha = 0.5$ and $\Delta_R = 5 \times 10^{-4} E_0$ at $\alpha = 0.7$. In each instance this roughly corresponds to $E_{Jd} \sim \sqrt{(2e)^2 E_J / C} / 20$. The $M_{cs} = 7$ results are compared to the $M_{cs} = 1$ lineshape (12), at the same Kondo scale. Lines a $\sim 1/j$ and b $\sim 1/j^2$ are there to guide the eye.

each $|\Psi_n\rangle$ is a coherent state of the form (9) with variationally determined amplitudes p_n and displacements $f_k^{(n)}$. As M_{cs} is increased, $|\Psi\rangle$ rapidly converges to the exact ground state. Our technique, based on the exact many-body state, provides a powerful alternative to the usual numerical renormalization group calculations of the Kondo cloud [36, 38], which in contrast, requires a distinct computation for each spatial distance considered. The resulting correlation function χ_j for increasing values of the dissipation strength α is shown in Fig. 3. The cloud polarization χ_j still decays quadratically $\sim -Z(E_0/\Delta_R)/j^2$ at the largest distances, but with a Kondo energy Δ_R that is renormalized downwards from the value predicted by (10) (our data at $\alpha = 0.7$ shows a renormalization of Δ_R by a factor $\sim 1/4$). At $j \sim E_0/\Delta_R$, a broad cross-over is visible. In the intermediate distance universal regime, i.e. $\sqrt{C/C_g} \ll j \ll E_0/\Delta_R$, the correlation function χ_j decays slower than $1/j$. At strong dissipation (large α), our results are consistent with the perturbative prediction $\chi_j \sim -1/[j \ln(j)^2]$, but for the realistic system size considered, it is difficult to achieve the extreme separation of scales between $\sqrt{C/C_g}$ and E_0/Δ_R that is required to identify this lineshape unambiguously. We compare the converged results with $M_{cs} = 7$ coherent states to the analytical $M_{cs} = 1$ result (12), but with the true Kondo scale Δ_R , rather than the $M_{cs} = 1$ estimate (10). It is very interesting that, as the dissipation strength increases, a noticeable difference develops at intermediate distances between the line shapes predicted by the simple $M_{cs} = 1$ approximation and the fully converged $M_{cs} = 7$

result. These differences originate from subtle entanglement within the states in the bath [12]. Indeed, contrary to the simple Ansatz (9) that is based on a single (multi-mode) coherent state, the environmental wavefunction in the multiple coherent state expansion cannot be factorized.

Despite the quantitative differences in the intermediate distance universal regime, it is very surprising how accurate the simple Ansatz (9) turns out to be, highlighting the unexpected simplicity of the many-body ground state of such a complicated and widely investigated Hamiltonian as the spin-boson model (2). Our results indicate that strongly interacting quantum problems display a hidden structure that is more generic than the specific model studied in this Letter, since fermionic impurity problems should show similar properties. With the rapid advances in circuit QED architecture, we believe that future experiments following our proposal to probe the Josephson-Kondo cloud will be able to reveal the simple correlations that are at the heart of these many-body states.

Stimulating discussions with Olivier Buisson, Benedikt Lechtenberg and Nicolas Roch are gratefully acknowledged. This work is based on research supported in part by the National Research Foundation of South Africa (Grant Number 90657).

-
- [1] Y. Makhlin, G. Schön, and A. Shnirman, *Rev. Mod. Phys.* **73**, 357 (2001).
 - [2] R. J. Schoelkopf and S. M. Girvin, *Nature* **451**, 664 (2008).
 - [3] D. Zueco, C. Fernández-Juez, J. Yago, U. Naether, B. Peropadre, J. J. García-Ripoll, and J. J. Mazo, *Supercond. Sci. Technol.* **26** 074006 (2013).
 - [4] P. Jung, A. V. Ustinov, S. M. Anlage, *Supercond. Sci. Technol.* **27**, 073001 (2014).
 - [5] T. Niemczyk, F. Deppe, H. Huebl, E.P. Menzel, F. Hocke, M.J. Schwarz, J.J. García-Ripoll, D. Zueco, T. Hümmer, E. Solano, A. Marx, and R. Gross, *Nat. Phys.* **6**, 772 (2010).
 - [6] P. Forn-Díaz, J. Lisenfeld, D. Marcos, J. García-Ripoll, E. Solano, C. Harmans, and J. Mooij, *Phys. Rev. Lett.* **105**, 237001 (2010).
 - [7] O. Astafiev, A.M. Zagoskin, A.A. Abdumalikov, Y.A. Pashkin, T. Yamamoto, K. Inomata, Y. Nakamura, and J.S. Tsai, *Science* **327**, 840 (2010).
 - [8] A.A. Abdumalikov, O. Astafiev, A.M. Zagoskin, Y.A. Pashkin, Y. Nakamura, and J.S. Tsai, *Phys. Rev. Lett.* **104**, 193601 (2010).
 - [9] E. Sánchez-Burillo, D. Zueco, J. García-Ripoll, L. Martn-Moreno, *Phys. Rev. Lett.* **113**, 263604 (2014).
 - [10] K. Le Hur, *Phys. Rev. B* **85**, 140506 (2012).
 - [11] M. Goldstein, M. H. Devoret, M. Houzet, and L. I. Glazman, *Phys. Rev. Lett.* **110**, 017002 (2013).
 - [12] S. Bera, S. Florens, H. U. Baranger, N. Roch, A. Nazir, and A. W. Chin, *Phys. Rev. B* **89**, 121108(R) (2014).
 - [13] A. C. Hewson, *The Kondo Problem to Heavy Fermions* (Cambridge University Press, Cambridge, UK, 1993).

contains the set of capacitances of the whole system, whereas the matrix

$$\hat{V} = E_J \begin{pmatrix} 0 & 0 & & & \\ 0 & 1 & -1 & & \\ & -1 & 2 & -1 & \\ & & -1 & 2 & -1 \\ & & & \ddots & \ddots & \ddots \end{pmatrix} \quad (\text{S3})$$

describes the Josephson couplings in the leads only. The indexing convention is such that the upper-left entries of these matrices are labeled by M_{00} and V_{00} . One would like to express H_0 as a bath of independent oscillators that are linearly coupled to the impurity at site 0. This is achieved by expressing the set of harmonic variables in terms of bosonic operators:

$$p_m = \frac{1}{\sqrt{2}} \int_0^{+\infty} dk \theta_{mk} (b_k + b_k^\dagger) \quad m = 1, 2, \dots, +\infty \quad (\text{S4})$$

$$x_m = \frac{i}{\sqrt{2}} \int_0^{+\infty} dk \xi_{mk} (b_k - b_k^\dagger) \quad m = 1, 2, \dots, +\infty \quad (\text{S5})$$

where ξ_{mk} and θ_{mk} are real numbers. Note that we adopted the unusual (but legitimate) convention of ascribing the momentum variable (and not the position variable) to the sum of creation and annihilation operators. Since the qubit is capacitively coupled to its environment through the momentum p_0 , this choice will result in the standard form of the spin boson Hamiltonian. We also stress that the coordinates (x_0, p_0) at the end of the chain are not part of this decomposition, which will facilitate the later projection onto the two-level system. A first important relation follows from (S4-S5) by imposing the commutation relation $[x_m, p_n] = i\delta_{m,n}$ and assuming standard algebra of the bosonic operators, namely $[b_k, b_{k'}] = 0$, $[b_k, b_{k'}^\dagger] = \delta(k - k')$:

$$\int_0^{+\infty} dk \xi_{mk} \theta_{nk} = \delta_{m,n}. \quad (\text{S6})$$

Normal mode diagonalization of the chain

Let's focus first on the chain part of H_0 which contains the sites $m = 1, 2, \dots, +\infty$ only, and impose that it is diagonalized by the bosonic operators:

$$H_0^{\text{chain}} = \frac{1}{2} \sum_{m,n \neq 0} p_m \left(\hat{M}^{-1} \right)_{mn} p_n + \frac{1}{2} \sum_{m,n \neq 0} x_m V_{mn} x_n \equiv \int_0^{+\infty} dk \omega_k b_k^\dagger b_k, \quad (\text{S7})$$

with ω_k the positive frequencies of the normal modes. Using the decomposition (S4-S5), this provides several constraints on the set of unknown parameters:

$$0 = \sum_{m,n \neq 0} \left[\theta_{mk} \left(\hat{M}^{-1} \right)_{mn} \theta_{nk'} - \xi_{mk} V_{mn} \xi_{nl'} \right] \quad (\text{S8})$$

$$2\omega_k \delta(k - k') = \sum_{m,n \neq 0} \left[\theta_{mk} \left(\hat{M}^{-1} \right)_{mn} \theta_{nk'} + \xi_{mk} V_{mn} \xi_{nl'} \right]. \quad (\text{S9})$$

One can then take the sum and differences of Eq. (S8-S9), and integrate them respectively with $\int_0^{+\infty} dk \xi_{pk'}$ and with $\int_0^{+\infty} dk \theta_{pk'}$. Using the orthogonality condition (S6), one readily gets:

$$\sum_{m \neq 0} \theta_{mk} \left(\hat{M}^{-1} \right)_{mp} = \omega_k \xi_{pk} \quad (\text{S10})$$

$$\sum_{m \neq 0} \xi_{mk} V_{mp} = \omega_k \theta_{pk}. \quad (\text{S11})$$

In order to write the above equations as full matrix products, we extend the variables to the range $m = 0, 1, \dots, +\infty$, and define the vectors $\vec{\xi}_k = (\xi_{0k}, \xi_{1k}, \xi_{2k}, \dots)$ and $\vec{\theta}_k = (\theta_{0k}, \theta_{1k}, \theta_{2k}, \dots)$. Noting that $V_{0p} = 0$ and with the condition

$\theta_{0k} = 0$, we can write:

$$\hat{M}^{-1}\vec{\theta}_k = \omega_k \vec{\xi}_k \quad (\text{S12})$$

$$\hat{V}\vec{\xi}_k = \omega_k \vec{\theta}_k. \quad (\text{S13})$$

This results in an eigenvalue equation $\hat{M}^{-1}\hat{V}\xi_k = \omega_k^2 \xi_k$, which can be rewritten in the explicit form (that avoids inverting explicitly the matrix \hat{M}):

$$\hat{V}\vec{\xi}_k = \omega_k^2 \hat{M}\vec{\xi}_k. \quad (\text{S14})$$

This gives a set of conditions, for the different cases $m = 0$, $m = 1$, and $m \geq 2$:

$$\xi_{0k} = \frac{C_d}{C_{gd} + C_d} \xi_{1k} \quad (\text{S15})$$

$$\xi_{2k} = \left[1 - \frac{C_{\text{eff}}\omega_k}{(2e)^2 E_J - C\omega_k^2} \right] \xi_{1k} \quad (\text{S16})$$

$$\xi_{m+1,k} = 2 \frac{(2e)^2 E_J - (C + C_g/2)\omega_k^2}{(2e)^2 E_J - C\omega_k^2} \xi_{mk} - \xi_{m-1,k} \quad (\text{S17})$$

with $C_{\text{eff}} = C_g + C_{gd}C_d/(C_{gd} + C_d)$. Now we exploit the fact that the Josephson chain is uniform except at the first two sites. We thus introduce scattering states that we parametrize as follows:

$$\xi_{mk} = N_k \cos[k(m - 1/2) - \delta_k] \quad m = 1, 2, \dots, +\infty \quad (\text{S18})$$

with amplitude N_k and phase shift δ_k to be determined. Inserting the above expression into Eq. (S17), we readily find the eigenfrequency:

$$\omega_k^2 = \frac{4(2e)^2 E_J \sin^2(k/2)}{C_g + 4C \sin^2(k/2)}. \quad (\text{S19})$$

The phase shift is then determined from condition (S16), which reads:

$$\cos\left(\frac{3k}{2} - \delta_k\right) = \left[1 - \frac{C_{\text{eff}}\omega_k^2}{(2e)^2 E_J - C\omega_k^2} \right] \cos\left(\frac{k}{2} - \delta_k\right). \quad (\text{S20})$$

After some trigonometric manipulation and using Eq. (S19), one finds the simple condition:

$$\sin(\delta_k) = \left[1 - \frac{C_g}{C_{\text{eff}}} \right] \sin(\delta_k - k), \quad (\text{S21})$$

which is solved explicitly as:

$$\delta_k = \arctan \left[\frac{\left(1 - \frac{C_g}{C_{\text{eff}}}\right) \sin(k)}{\left(1 - \frac{C_g}{C_{\text{eff}}}\right) \cos(k) - 1} \right]. \quad (\text{S22})$$

It is useful to establish an inverse relation between the harmonic variables and bosonic operators. Using (S6), it is straightforward to check that the relations (S4-S5) can be inverted by:

$$b_k = \frac{1}{\sqrt{2}} \sum_{m=1}^{\infty} [\xi_{mk} p_m - i\theta_{mk} x_m] \quad (\text{S23})$$

$$b_k^\dagger = \frac{1}{\sqrt{2}} \sum_{m=1}^{\infty} [\xi_{mk} p_m + i\theta_{mk} x_m]. \quad (\text{S24})$$

One is equipped now to determine the normalization factor N_k , which follows from the commutation relation $[b_k, b_{k'}^\dagger] = \delta(k - k')$. This relation is equivalent to the condition $\vec{\theta}_k \cdot \vec{\xi}_{k'} = \delta(k - k')$, which can be rewritten as:

$$\sum_{m,n \neq 0} \xi_{mk} V_{mn} \xi_{nk'} = \delta(k - k'). \quad (\text{S25})$$

From the explicit expression of \hat{V} and the recursion relations (S16-S17), one gets:

$$\delta(k - k') = 4 \frac{E_J}{\omega_k} \sin^2(k/2) \left[\frac{C_{\text{eff}} - C_g}{C_g} \xi_{1k} \xi_{1k'} + \sum_{m=1}^{+\infty} \xi_{mk} \xi_{mk'} \right]. \quad (\text{S26})$$

Finally, using expression (S18) and the following standard algebraic identities $\sum_{m=1}^{\infty} \cos(mk) = \pi\delta(k) - 1/2$ and $\sum_{m=1}^{\infty} \sin(mk) = 1/[2 \tan(k/2)]$, one finds:

$$\delta(k - k') = 2\pi \frac{E_J}{\omega_k} \sin^2(k/2) N_k^2 \delta(k - k') + \text{Finite Terms}, \quad (\text{S27})$$

where we have singled out the delta-function contribution. Let us prove that the finite terms are actually zero, which implies the choice of normalization:

$$N_k = \frac{1}{\sin(k/2)} \sqrt{\frac{\omega_k}{2\pi E_J}}. \quad (\text{S28})$$

For this purpose, let us show that $\vec{\theta}_k \cdot \vec{\xi}_{k'} = 0$ for all $k \neq k'$. The proof relies on equations (S12-S13):

$$\omega_{k'}^2 \vec{\theta}_k \cdot \vec{\xi}_{k'} = \vec{\theta}_k \cdot \hat{M}^{-1} \hat{V} \vec{\xi}_{k'} = \left(\hat{V} \hat{M}^{-1} \vec{\theta}_k \right)^T \xi_{k'} = \omega_k^2 \vec{\theta}_k \cdot \vec{\xi}_{k'}. \quad (\text{S29})$$

Since ω_k^2 is a monotonous function of k , the scalar product $\vec{\theta}_k \cdot \vec{\xi}_{k'}$ indeed vanishes for $k \neq k'$.

Expression for the full Hamiltonian

The impurity part of the quadratic Hamiltonian (S1) related to the site $m = 0$ reads:

$$H_0^{\text{imp}} = \frac{1}{2} \left(\hat{M}^{-1} \right)_{00} p_0^2 + p_0 \sum_{m=1}^{+\infty} \left(\hat{M}^{-1} \right)_{0m} p_m. \quad (\text{S30})$$

Using Eq. (S4) and Eq. (S10), we finally obtain an exact and remarkably compact expression for the full Hamiltonian in terms of the normal modes and of the variables at the first two sites of the Josephson chain:

$$H = \frac{1}{2} \left(\hat{M}^{-1} \right)_{00} p_0^2 + \int_0^\pi dk \omega_k b_k^\dagger b_k + \frac{p_0}{\sqrt{2}} \int_0^\pi dk \omega_k \xi_{0k} (b_k + b_k^\dagger) - E_J d \cos(x_0 - x_1). \quad (\text{S31})$$

To get rid of the factors containing x_1 , we perform a unitary transformation $\tilde{H} = U H U^\dagger$, with $U = e^{ip_0 x_1}$. The transformed Hamiltonian reads

$$\tilde{H} = \frac{1}{2m} p_0^2 + \int_0^\pi dk \omega_k b_k^\dagger b_k - \frac{1}{\sqrt{2}} p_0 \int_0^\pi dk \omega_k \xi_{0k} (b_k^\dagger + b_k) - \frac{E_J d}{2} [e^{ix_0} + e^{-ix_0}] \quad (\text{S32})$$

where

$$\frac{1}{m} = \left(\hat{M}^{-1} \right)_{00} + \left(1 - \frac{2C_d}{C_d + C_{dg}} \right) \int_0^\pi dk \omega_k \xi_{1k}^2. \quad (\text{S33})$$

Now we assume that we are at a degeneracy point of the uncoupled impurity, and project the impurity part of the Hilbert space onto the two degenerate states. This results in $p_0 \rightarrow \sigma_z/2$ and $(e^{ix_0} + e^{-ix_0}) \rightarrow \sigma_x$. It produces a spin-boson Hamiltonian (where again, we drop constant terms)

$$\tilde{H} \simeq \int_0^\pi \omega_k b_k^\dagger b_k - \frac{1}{\sqrt{2}} \frac{C_{dg}}{C_{dg} + C_d} \int_0^\pi dk \omega_k \xi_{1k} (b_k^\dagger + b_k) \frac{\sigma_z}{2} - E_J d \frac{\sigma_x}{2} \quad (\text{S34})$$

For $k \ll \sqrt{C_g/C}$,

$$\omega_k \simeq E_0 k \quad (\text{S35})$$

$$\xi_{1k} \simeq 2 \sqrt{\frac{E_0}{2\pi E_J k}} \quad (\text{S36})$$

with $E_0 = \sqrt{(2e)^2 E_J / C_g}$. We can thus identify the Ohmic spin-boson model parameter

$$\alpha = \frac{1}{2\pi} \left(\frac{C_{dg}}{C_{dg} + C_d} \right)^2 \frac{E_0}{E_J}. \quad (\text{S37})$$

From the point of view of the impurity, α is the effective fine structure constant when the photonic modes of the vacuum are replaced by the plasmonic modes of the superconducting environment. This interpretation is confirmed by noting that the fine structure constant in vacuum $\alpha_{\text{vac.}} = (e^2/2h)Z_{\text{vac.}}$ (with e the electron charge and h Planck's constant) is fixed to the small 1/137 value by the vacuum impedance $Z_{\text{vac.}} = \sqrt{\mu_0/\epsilon_0} \simeq 377 \Omega$. In transmission lines, an effective fine structure constant can thus be defined as $\alpha = (e^2/2h)Z$ from the environmental impedance Z , typically related to a ratio from line inductances L and shunt capacitances C , $Z = \sqrt{L/C}$. In superconducting circuits, the Josephson inductance is given by $L = (h/4\pi e)^2 1/E_J$, so that we indeed recover Eq. (S37) up to numerical and geometrical factors.

Connection between the magnetic Josephson-Kondo screening cloud and the Kondo screening cloud

Here we explain the mathematical correspondence between the Kondo screening cloud and the Josephson-Kondo screening cloud. For a spin 1/2 magnetic moment at $x = 0$, quenched in a one dimensional electron gas, the longitudinal Kondo screening cloud is defined as

$$X^{\parallel}(x) = 4 \langle S_z^{\text{imp}} S_z^{\text{el}}(x) \rangle. \quad (\text{S38})$$

Here S_z^{imp} is the z -component of the impurity spin, and $S_z^{\text{el}}(x)$ is the z -component of the electron spin density at x . The cloud can be decomposed into

$$X^{\parallel}(x) = X_0^{\parallel}(x) + \cos(2k_F x) X_{2k_F}^{\parallel}(x), \quad (\text{S39})$$

where $X_0^{\parallel}(x)$ and $X_{2k_F}^{\parallel}(x)$ vary slowly on the scale of the Fermi wavelength $2\pi/k_F$. Using the well-known mapping between the Kondo model and the spin-boson model,[1, 2] the component $X_0^{\parallel}(x)$ can be expressed as

$$aX_0^{\parallel}(x) = \frac{1}{\pi} \int_0^{\infty} dq X_q(x) \left\langle \sigma_z \frac{(b_q^{\dagger} + b_q)}{\sqrt{2}} \right\rangle \quad (\text{S40})$$

where

$$X_q(x) = \sqrt{q} e^{-q/2} \cos\left(\frac{qx}{a}\right). \quad (\text{S41})$$

Here $1/a$ is the ultra-violet scale in the problem (of the order of k_F), q is dimensionless, and the expectation value is with respect to the ground state of the spin-boson model. Comparing this expression to the expression (7) for χ_j in the main text, we see that the two integrands have the same low q behavior. Thus, the $0k_F$ component of the Kondo cloud for $x \gg a$, corresponds to the Josephson-Kondo cloud for $j \gg \sqrt{C/C_g}$. Explicitly, the correspondence is

$$\begin{aligned} aX_0^{\parallel}(x) &\leftrightarrow \sqrt{\frac{2E_0}{\pi E_J}} \chi_j \\ \frac{x}{a} &\leftrightarrow j - \frac{1}{2} + \delta l \end{aligned} \quad (\text{S42})$$

At distances where the correspondence is accurate, the profile of the cloud is universal. This can be seen analytically in the regime of small to moderate dissipation, where the exact Josephson-Kondo cloud is given by Eq. (11) in the main text. As pointed out there, it depends on all the microscopic parameters of the device. However, for j sufficiently larger than $\sqrt{C/C_g}$, but not necessarily larger than $1/\Delta_R$, the integrand of Eq. (11) in the main text can be approximated as

$$\frac{\cos[k(j - 1/2 + \delta l)]}{E_0 k + \Delta_R}, \quad (\text{S43})$$

due to rapid oscillations when $k \gtrsim 1/j$. For the same reason, the upper bound of the integral can be extended from π to ∞ . Under this approximation, the integral evaluates to

$$\chi_j = -Z \operatorname{Re} \left\{ e^{-i \frac{\Delta_R}{E_0} (j-1/2+\delta l)} \Gamma \left[0, -i \frac{\Delta_R}{E_0} (j-1/2+\delta l) \right] \right\}, \quad (\text{S44})$$

where $\Gamma(a, z)$ is the incomplete Gamma function and Z is as defined in Eq. (13) in the main text. We have said that under the assumptions we make about capacitances, δl is small. In the same regime, the Kondo scale Δ_R is small relative to the ultra-violet scale E_0 . This implies that χ_j varies slowly on the scale of $\delta l - 1/2$, and we can therefore replace $j - 1/2 + \delta l \rightarrow j$ in the above equation. In this way, we obtain Eq. (12) in the main text.

The harmonic chain

In the main text we argued that the non-trivial physics we investigate is generated by the anharmonic term $-E_{Jd} \cos(\phi_0 - \phi_1)$ in the Hamiltonian (1). Specifically, we want to show that without the anharmonicity, correlations decay far more rapidly than with the anharmonicity. In order to justify these statements and make them more precise, we study here the harmonic chain. That is, we consider the regime $E_{Jd} \gg (2e)^2/(C_d + C_{gd})$, where the cosine term in the Hamiltonian (1) can be expanded to quadratic order in the phase difference $\phi_0 - \phi_1$, yielding a harmonic chain

$$H_H = \frac{(2e)^2}{2} \sum_{i,j=0}^{\infty} (n_i - \bar{n}_i) \left(\hat{C}^{-1} \right)_{ij} (n_j - \bar{n}_j) + \frac{E_J}{2} \sum_{i=1}^{\infty} (\phi_i - \phi_{i+1})^2 + \frac{E_{Jd}}{2} (\phi_0 - \phi_1)^2. \quad (\text{S45})$$

The Hamiltonian is again diagonalized by defining bosonic operators b_k and b_k^\dagger , for $k \in [0, \pi]$, such that

$$b_k = \frac{1}{\sqrt{2}} \sum_{j=0}^{\infty} [\xi_{jk} (n_j - \bar{n}_j) - i \theta_{jk} \phi_j]. \quad (\text{S46})$$

As before, ξ_{jk} is obtained from the classical equations of motion. The presence of the quadratic Josephson coupling between sites $i = 0$ and $i = 1$ modifies the expressions for ξ_{jk} as follows. The relation between ξ_{0k} and ξ_{1k} now reads

$$\xi_{0k} = (1 - F_k) \xi_{1k}, \quad F_k = \frac{\omega_k^2 C_{gd}}{\omega_k^2 (C_{gd} + C_d) - (2e)^2 E_{Jd}}. \quad (\text{S47})$$

For $j \geq 1$, the form of ξ_{jk} is still

$$\xi_{jk} = N_k \cos[k(j-1/2) - \delta_k]. \quad (\text{S48})$$

In the last two equations, the form of ω_k and N_k are unchanged from what they were before, but the phase shift δ_k is obviously affected by the Josephson coupling between sites $i = 0$ and $i = 1$. It is now given by

$$\tan(\delta_k) = \frac{\sin k}{\cos k - 1 - \frac{C_g}{C_{gd}(1-F_k)}}. \quad (\text{S49})$$

The relationship between $\vec{\theta}_k$ and $\vec{\xi}_k$ is still given by (S12) and (S13), but in (S13), one has to remember to include the extra E_{Jd} couplings, i.e. $V_{00} = E_{Jd}$, $V_{11} = E_{Jd} + E_J$, and $V_{01} = V_{10} = -E_{Jd}$. The ground state of the harmonic chain (S45) is the bosonic vacuum $|0\rangle$ defined by the condition that $b_k |0\rangle = 0$ for all k in $[0, \pi]$.

For the correlator χ_j one then obtains

$$\begin{aligned} \chi_j &= \langle 0 | (n_0 - \bar{n}_0)(n_j - \bar{n}_j) | 0 \rangle \\ &= \frac{1}{2} \int_0^\pi dk \theta_{0k} \theta_{jk} \\ &= -\frac{E_J}{\pi} \int_0^\pi dk \frac{F_k}{\omega_k} \cos(k/2 - \delta_k) \cos[k(j-1/2) - \delta_k], \end{aligned} \quad (\text{S50})$$

the last line being valid for $j \geq 2$. Note that, while F_k diverges at the point $k = k_*$ such that $\omega_{k_*}^2 = (2e)^2 E_{Jd}/(C_{gd} + C_d)$, the product $F_k \cos(k/2 - \delta_k)$ remains finite at $k = k_*$, so that the integrand in the last line of (S50) is a smooth

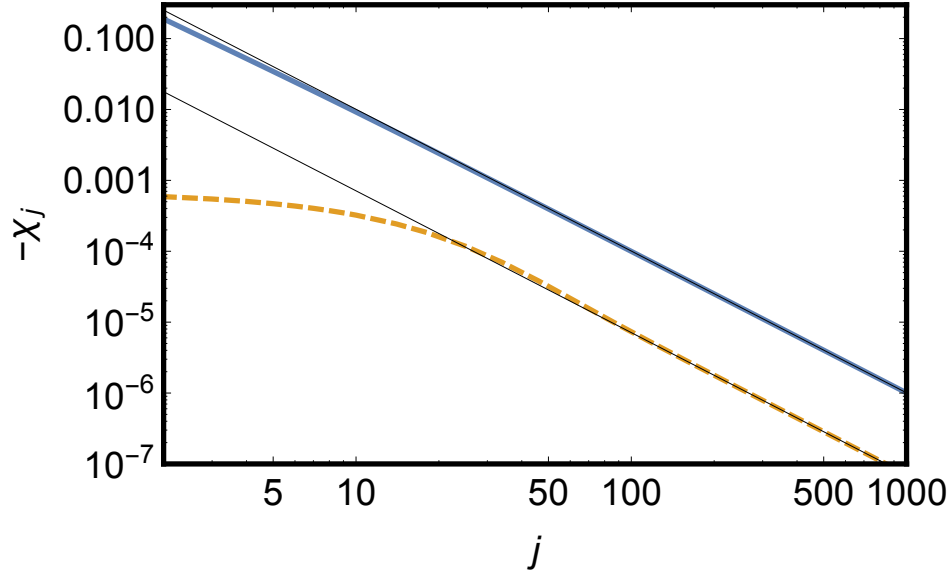


FIG. S1. The correlation function χ_j for the harmonic chain, calculated from Formula (S50). The dashed curve shows the result for weak dissipation (large C), and was calculated for $C_d = C_{gd} = C_g$, $E_{Jd} = 10(2e)^2/C_g$, and $E_J = 10(2e)^2/(2C + C_g)$. For the anharmonic impurity system (i.e. a much smaller value of E_{Jd}), the remaining parameter values would have corresponded to $\alpha = 0.035$. The solid curve shows the result for strong dissipation (small C), and was calculated for $C = C_d = C_g/100$, $C_{gd} = C_g$, and $E_{Jd} = E_J = 10(2e)^2/C_g$. For the anharmonic impurity system (i.e. a much smaller value of E_{Jd}), in this case, the remaining parameter values would have corresponded to $\alpha = 0.5$. For both the solid and the dashed curve, a thin solid line indicates $1/j^2$ with the prefactor predicted by Formula (S52).

function of k . At sufficiently large j , the slowly varying factor $F_k \cos(k/2 - \delta_k)/\omega_k$ can be evaluated to linear order in k , yielding

$$\begin{aligned} \chi_j &\simeq \frac{1}{\pi} \frac{E_0 C_{gd}}{(2e)^2} \int_0^\pi dk k \cos[k(j - 1/2) - \delta_k], \\ &= \frac{1}{\pi} \frac{E_0 C_{gd}}{(2e)^2} \partial_j \int_0^\pi dk \sin[k(j - 1/2) - \delta_k], \end{aligned} \quad (\text{S51})$$

At large j , the phase shift δ_k dephases the contribution from evaluating the integral without the phase shift at $k = \pi$. Replacing $j - 1/2 \rightarrow j$, which is allowed within the accuracy to which we evaluated the integral, we then find

$$\chi_j \simeq \frac{1}{\pi} \frac{E_0 C_{gd}}{(2e)^2} \partial_j \left[-\frac{1}{j} \cos(jk) \right]_0^\pi = -\frac{E_0 C_{gd}}{\pi(2e)^2} \frac{1}{j^2}. \quad (\text{S52})$$

For the anharmonic system that we studied in the main text, we found on the other hand

$$\chi_j \simeq -Z \left(\frac{E_0}{\Delta_R} \right)^2 \frac{1}{j^2} = -\frac{(2e)^2}{2\Delta_R(C_d + C_{gd})} \times \frac{E_0 C_{gd}}{\pi(2e)^2} \frac{1}{j^2}. \quad (\text{S53})$$

At strong dissipation, this results in a correlation function that is larger than in the harmonic case by a factor proportional to the inverse of the (exponentially small) Kondo energy.

Next we ask at what distance the $1/j^2$ behavior predicted in Formula (S52) sets in. For the harmonic chain, the $1/j^2$ decay breaks down below a distance $j \sim 1/k_0$, where k_0 is the value of k where the k^3 term in the Taylor expansion of $F_k \cos(k/2 - \delta_k)/\omega_k$ in the integrand of (S50) becomes important. Under the assumptions we make about the sizes of capacitances, it follows that $k_0 \sim \min\{\sqrt{C_g/C}, 1\}$. Hence, for the harmonic chain, $\chi_j \sim 1/j^2$ behavior is seen for $j \gg \max\{\sqrt{C/C_g}, 1\}$. In contrast, for the anharmonic impurity, we saw in the main text that there is an intermediate regime $\sqrt{C/C_g} \ll j \ll E_0/\Delta_R$, where correlations decay far more slowly.

We also note the following. In the anharmonic impurity problem, one increases the dissipation strength α to values of order 1 by decreasing C , while keeping $E_J(2C + C_g)/(2e)^2$ large. This has the effect of decreasing Δ_R , and hence the region of the onset of $1/j^2$ decay is shifted to larger j . In the harmonic problem, increasing C tends

to have the opposite effect, namely, it shifts the onset of $1/j^2$ decay to smaller j . This is illustrated in Fig. S1, where the exact formula (S50) and the large j asymptotic formula (S52) for χ_j in the harmonic system are compared, for fixed $E_J(2C + C_g)/(2e)^2$, but different C . These results justify the statement we make in the main text that the Josephson-Kondo cloud is a hallmark of the strong coupling between a two-level system and its macroscopic environment.

-
- [1] T. A. Costi and G. Zaránd, Phys. Rev. B **59**, 12398, (1999).
[2] G. Kotliar and Q. Si, Phys. Rev. B **53**, 12373, (1996).